



Identification of metastasis driver genes by massive parallel sequencing of successive steps of breast cancer progression

Krøigård, Anne Bruun; Larsen, Martin Jakob; Lænkholm, Anne-Vibeke; Knoop, Ann S; Jensen, Jeanette Dupont; Bak, Martin; Mollenhauer, Jan; Thomassen, Mads; Kruse, Torben A

Published in:
PLoS ONE

DOI:
[10.1371/journal.pone.0189887](https://doi.org/10.1371/journal.pone.0189887)

Publication date:
2018

Document version
Publisher's PDF, also known as Version of record

Document license:
[CC BY](#)

Citation for published version (APA):
Krøigård, A. B., Larsen, M. J., Lænkholm, A-V., Knoop, A. S., Jensen, J. D., Bak, M., ... Kruse, T. A. (2018). Identification of metastasis driver genes by massive parallel sequencing of successive steps of breast cancer progression. *PLoS ONE*, 13(1), [e0189887]. <https://doi.org/10.1371/journal.pone.0189887>

RESEARCH ARTICLE

Identification of metastasis driver genes by massive parallel sequencing of successive steps of breast cancer progression

Anne Bruun Krøigård^{1,2*}, Martin Jakob Larsen^{1,2}, Anne-Vibeke Lænkholm³, Ann S. Knoop⁴, Jeanette Dupont Jensen⁵, Martin Bak⁶, Jan Mollenhauer^{7,8}, Mads Thomassen^{1,2,7}, Torben A. Kruse^{1,2,7}

1 Department of Clinical Genetics, Odense University Hospital, Odense, Denmark, **2** Human Genetics, Institute of Clinical Research, University of Southern Denmark, Odense, Denmark, **3** Department of Pathology, Slagelse Hospital, Slagelse, Denmark, **4** Department of Oncology, Rigshospitalet, Copenhagen, Denmark, **5** Department of Oncology, Odense University Hospital, Odense, Denmark, **6** Department of Pathology, Odense University Hospital, Odense, Denmark, **7** Lundbeckfonden Center of Excellence NanoCAN, University of Southern Denmark, Odense, Denmark, **8** Molecular Oncology Group, Institute of Molecular Medicine, University of Southern Denmark, Odense, Denmark

* anne.kroeigaard@rsyd.dk



OPEN ACCESS

Citation: Krøigård AB, Larsen MJ, Lænkholm A-V, Knoop AS, Jensen JD, Bak M, et al. (2018) Identification of metastasis driver genes by massive parallel sequencing of successive steps of breast cancer progression. PLoS ONE 13(1): e0189887. <https://doi.org/10.1371/journal.pone.0189887>

Editor: Rajeev Samant, University of Alabama at Birmingham, UNITED STATES

Received: July 14, 2017

Accepted: December 4, 2017

Published: January 2, 2018

Copyright: © 2018 Krøigård et al. This is an open access article distributed under the terms of the [Creative Commons Attribution License](https://creativecommons.org/licenses/by/4.0/), which permits unrestricted use, distribution, and reproduction in any medium, provided the original author and source are credited.

Data Availability Statement: All relevant data are within the paper and its Supporting Information files.

Funding: The project received funding from: Odense University Hospital Free Research Fund, Harboefonden, Aase og Ejnar Danielsen Fond, Fabrikant Einar Willumsens Mindelegat, Grosserer M. Brogaard og Hustrus Mindefond, Kong Christian Den Tiendes Fond, Dagmar Marshalls Fond, Axel Muusfeldts Fond, Kræftfonden,

Abstract

Cancer results from alterations at essential genomic sites and is characterized by uncontrolled cell proliferation, invasion and metastasis. Identification of driver genes of metastatic progression is essential, as metastases, not primary tumors, are fatal. To gain insight into the mutational concordance between different steps of malignant progression we performed exome sequencing and validation with targeted deep sequencing of successive steps of malignant progression from pre-invasive stages to asynchronous distant metastases in six breast cancer patients. Using the ratio of non-synonymous to synonymous mutations, a surprisingly large number of cancer driver genes, ranging between 3 and 145, were estimated to confer a selective advantage in the studied primary tumors. We report a substantial amount of metastasis specific mutations and a number of novel putative metastasis driver genes. Most notable are the *DCC*, *ABCA13*, *TIAM2*, *CREBBP*, *BCL6B* and *ZNF185* genes, mainly mutated exclusively in metastases and highly likely driver genes of metastatic progression. We find different genes and pathways to be affected at different steps of malignant progression. The Adherens junction pathway is affected in four of the six studied patients and this pathway most likely plays a vital role in the metastatic process.

Introduction

Cancer evolves through the stochastic, cumulative acquisition of driver mutations disrupting key pathways leading to the hallmarks of cancer [1]. A cancer driver mutation confers a selective advantage, while passenger mutations are coexisting mutations in the successfully expanding clones [2]. The cancer genome evolves dynamically influenced by the generation of additional mutations and selective forces acting on cancer clones, the latter being time and site dependent. The term *oncogene addiction* [3] describes the cancer cell dependence of particular

Raimond og Dagmar Ringgård-Bohns Fond, Grete og Sigurd Pedersens Fond, Syddansk Universitets Forskningsfond, Poul og Ellen Hertz' Fond, Fonden til Lægevidenskabens Fremme, Grosserer A.V. Lykfeldt og Hustrus Legat, Familien Hede Nielsens Fond, Lykfeldts Legat, Dansk Kræftforskningsfond, Ulla og Mogens Folmer Andersens Fond, Ingeniør K. A. Rohde og Hustrus Legat, Krista og Viggo Petersens Fond, the Lundbeckfonden Center of Excellence NanoCAN grant, and the DAWN 2020 project grant from the SDU2020 Excellence program, Danish Strategic Research Council, DBCG-TIBCAT.

Competing interests: The authors have declared that no competing interests exist.

driver genes for maintenance of the malignant phenotype and provides the rationale for targeted therapy. One of the major challenges in cancer genetics is to identify cancer driver genes.

Mutations in the coding region can be divided into synonymous, also known as silent mutations, and non-synonymous mutations. Typically, nucleotide substitutions in the third codon position are silent, whereas substitutions in the first and second codon positions result in an amino acid change. The ratio of non-synonymous to synonymous mutations (NS:S ratio) has been used as a reliable indicator of selection. Two factors influence the NS:S ratio, including the rate of creation and the selective forces acting on them. In the absence of selection, non-synonymous and synonymous mutations are equally likely to persist [4] and thus the NS:S ratio can indicate whether or not selection is occurring.

The metastatic process is highly complex and not yet fully understood. The main bottleneck for metastasis formation is believed to be colonization at the distant site [5]. A solid tumor is suggested to infiltrate into the circulatory system one million cancer cells per day [6] and tumor cells are found to disseminate systemically even from pre-invasive tissue [7]. Thus, additional genetic, epigenetic or host response events are needed in order to allow a disseminated tumor cell to create a metastatic lesion. Identification of specific driver genes of the metastatic process is to a large degree limited to the yet relatively few identified metastasis suppressor genes [8]. A reduced expression of a metastasis suppressor gene does not provide a selective advantage in the primary tumor, but plays a major role in the metastatic process [9]. Based on their level of participation in different steps of the metastatic process different classes of metastasis genes have been suggested: *metastasis initiation genes*, *metastasis progression genes* and *metastasis virulence genes* [10]. In addition to acquiring abilities like detachment, motility, invasion, intravasation, survival in the circulation and adaptation to new environment the malignant cell must be able to evade immune surveillance. Microenvironmental factors like acidity and hypoxia also provide selective forces upon the cancer clones [2]. Thus, the driving capacity of mutations is site dependent, inducing genetic disparity between a primary tumor and its metastases. Therapy-induced eradication of the dominant, chemotherapy- and anti-hormonal therapy sensitive clones serves to increase the selective pressure within the malignant cell population, leading to expansion of therapy-resistant clones. Hence, the location of a recurrence and treatment influences molding of the cancer genome at the distant site. Due to increasing genomic instability and stochastic events [9] cancer genome evolution must be expected to continue also in disseminated tumor cells after removal of the primary tumor.

In a recent study, including only two breast cancer patients, gene expression signatures, DNA copy number patterns and somatic mutation patterns were found to be highly similar across primary tumors and matched metastases [11]. In another study, including 11 patients, a high concordance of chromosomal rearrangements was found between primary tumors and matched metastases [12].

Mutational discordances between a primary tumor and its metastases may identify new driver genes of metastatic progression and provide insight into the biology underlying metastatic progression. In our study, we have used exome and deep targeted sequencing of pre-invasive stages, primary tumors, synchronous axillary lymph node (ALN) metastases and asynchronous distant metastases from six breast cancer patients to identify putative novel driver genes of metastatic progression and to identify pathways involved in metastasis.

Materials and methods

Patient material

The study includes successive tumor samples from six breast cancer patients with estrogen receptor (ER) positive invasive ductal carcinoma. Table 1 displays clinical information of the

Table 1. Patient characteristics.

| Pt ID | Age | Type | Primary size | ER | PR | HER 2 | MG | # pos LN | Relapse time | Treatment |
|-------|----------|------|-----------------------------------|-----|-----|-------|-----|----------|--------------|--|
| 4 | 72 years | IDC | 14 mm | pos | neg | A | II | 1/10 LN | 1.82 years | Surgery, adjuvant Letrozole. |
| 8 | 58 years | IDC | 50 mm | pos | pos | N | II | 15/15 LN | 4.05 years | 5 series of neo-adj. CEF, surgery, 4 series of Taxotere/Gemcitabine. Tamoxifen 2.5 years, then Arimidex, radiation therapy |
| 11 | 46 years | IDC | 25 mm | pos | pos | N | III | 1/15 LN | 2.57 years | Surgery, adjuvant 7 series of CEF, Tamoxifen, radiation therapy. |
| 15 | 66 years | IDC | 17 mm + 15 mm = multifokal | pos | pos | N | III | 17/18 LN | 3.90 years | Surgery, adjuvant Letrozole, radiation therapy. |
| 46 | 79 years | IDC | 10 mm and diffusely spread 110 mm | pos | neg | N | III | 5/20 LN | | Neo-adjuvant Letrozole, surgery. |
| 123 | 67 years | IDC | 23 mm | pos | neg | A | II | 5/11 LN | | Surgery. |

IDC: Invasive ductal carcinoma. ER: Estrogen receptor status. MG: Malignancy grade. PR: Progesterone receptor status. N: normal. A: amplified. CEF: Cyclofosamid, Epirubicin, 5- Fluoracil. LN: lymph nodes.

<https://doi.org/10.1371/journal.pone.0189887.t001>

patients. All patients had ALN metastases at the time of diagnosis and primary tumors from all patients and synchronous ALN metastases from five of the patients were secured during primary surgery and stored at -80°C until sample preparation. In three cases, also pre-invasive stages, Ductal Carcinoma in Situ (DCIS) were secured during primary surgery. In one case, Patient ID (PTID) 8, we had access to two different regions of DCIS and in one case, two different regions of primary tumor (PTID 4). In spite of adjuvant therapy, four of the patients experienced recurrence of the disease, with a median relapse time of 3.08 years, and asynchronous metastases were biopsied from bone, lymph node and in two cases liver, respectively. Haematoxylin-eosin sections of all tissue samples were reviewed by a certified pathologist, ensuring the diagnosis and a content of malignant cells of 50% at minimum. A start amount of 20–30 mg fresh frozen tissue (asynchronous metastasis 5 mg) was used for the purification process. Tissue disruption and homogenization was performed using TissueLyser (Qiagen) and purification of DNA was performed using AllPrep DNA/RNA Mini Kit (Qiagen). Matched normal tissue and the primary tumor of PT ID 8 were stored as formalin-fixed paraffin-embedded (FFPE) tissue. The FFPE blocks were cut in 30–40 sections of 10 µm and DNA extracted using AS1000 Maxwell 16 (Promega, USA).

Additional analyses of the data have been described in [13] and [14].

The patients provided written informed consent to participate in the study and for the data to be published. The study was approved by the Ethical Committee of Region Syddanmark and notified to the Danish Data Protection Agency.

Library construction and exome sequencing

One microgram of genomic DNA from each sample was randomly fragmented by focused acoustic shearing (Covaris inc.) according to Illumina's protocol. The fragment length was measured by Bioanalyzer (Agilent Technologies 2100), confirming a fragment length of 150–300 bp. Exome enrichment was performed with Illumina's TruSeq DNA Sample Preparation. Paired end sequencing of 2 x 100 bases was performed on the Illumina HiSeq 1500 platform. FASTQ files were aligned to the human reference genome GRCh37 (feb.2009) using the Novoalign v. 3 algorithm (www.novocraft.com) at default parameters. Removal of duplicate reads, recalibration and local realignment around indels were performed using Best Practices

pipeline v. 2.7 [15]. The result was a mean coverage rate in the exome region of 65–155 x in the tumor samples and 11–148 x in the matched normal samples (S1 Table).

Detection of putative somatic mutations for deep sequencing

On the exome sequencing data, somatic variant calling was performed using nine publicly available somatic variant callers: EB Call [16], Mutect [15], Seurat [17], Shimmer [18], Indelocator (<http://www.broadinstitute.org/cancer/cga/indelocator>), Somatic Sniper [17], Strelka [19], VarScan 2 [20] and Virmid [21]. The union of putative somatic mutations, except positions in intronic, intergenic, downstream and non-coding RNA intronic areas, reported by the nine somatic variant callers was used to select chromosomal candidate regions for targeted deep sequencing.

Validation with targeted deep sequencing

Target enrichment was performed using SureSelect DNA enrichment methodology (Agilent). A custom SureSelect enrichment kit was designed using the Agilent SureDesign application. Library construction and SureSelect enrichment were performed according to manufacturer's protocol and sequenced on the Illumina HiSeq 1500 platform with paired end sequencing 2 x 100 bases. Deep sequencing resulted in a mean coverage of 221–628 x of the targeted positions (S2 Table). Alignment and data preprocessing were performed as described previously. Variant calling were performed using VarScan 2 [20] version 2.3.6 (multisample setting). For each patient the following criteria were used: normal sample B Allele Frequency (BAF) less than 0.02, all samples should have a read depth of min. 50 x and BAF in one of the tumor samples should be 0.05 at minimum. For positions meeting those criteria, a mutation found with a BAF of 0.025 at minimum was included in other tumor samples if read depth exceeded 200 x. The variants were annotated with Annovar [22] and only exonic and splicing variants were included for further analysis. Known SNPs with a population allele frequency > 1% were excluded.

Subsequently, all identified somatic mutations within the coding region were manually curated, by visual inspection of the BAM files to remove false positive calls. Variants located in a repetitive area and variants with many adjacent variants were excluded, as they most likely result from systematic misalignment. Furthermore, unrelated BAM files were compared to the patient BAM files in order to identify error prone regions.

Pathway analysis of genes involved in different steps of malignant progression

The non-synonymous and splice site mutations were divided into three categories:

1. Mutations found exclusively in DCIS and primary tumors.
2. Mutations shared between primary tumors and metastases.
3. Mutations found exclusively in metastases.

Pathway analysis for overrepresentation of genes in KEGG gene sets (<http://www.genome.jp/kegg/>) were computed for each category of genes using the online tool Molecular Signatures Database by Broad Institute [23,24].

Identification of putative novel driver genes of metastatic progression

In order to prioritize among the many missense mutations, the iCAGES software tool (<http://icages.usc.edu>) was used in order to facilitate the distinction between driver and passenger

mutations. The iCAGES prioritization of putative cancer driver variants uses a radial Support Vector Machine (SVM) based on nine functional prediction tools (SIFT, PolyPhen-2, GERP+, FATHMM, Mutation Taster, Mutation Assessor, Siphy, PhyloP, LRT) which is trained on somatic non-synonymous SNVs from the Catalogue Of Somatic Mutations In Cancer (<http://cancer.sanger.ac.uk/cancergenome/projects/cosmic>) and the Uniprot databases (<http://www.uniprot.org>). The resulting radial SVM predicted score evaluates the cancer driver potential for each particular mutation. Additionally the iCAGES tool incorporates a Phenolyzer score evaluating the genetic-phenotypic association based on previous database knowledge (<http://phenolyzer.usc.edu>). A total weighed score, iCAGES score, ranks each mutation according to cancer driver potential.

Putative novel drivers of malignant progression were selected by the following criteria: Classified as a cancer driver gene by the iCAGES software or affected by a frameshift, stopgain or splicing mutation.

Results

Varying mutational concordance among the analyzed patients

A large variation in the number of mutations in the coding region of the studied patients was found. A total of 31–418 non-synonymous and splicing mutations and 13–113 synonymous mutations were identified by exome sequencing and validated by targeted deep sequencing in the six patients included in the study. The complete lists of validated somatic mutations in the coding region of the six studied patients are available in [S3–S8](#) Tables. Venn diagrams displaying the mutational concordance of non-synonymous and splice site mutations between different steps of malignant progression are shown in [Fig 1](#). The patients display varying degree of genetic concordance between different steps of progression. The majority of mutations are shared between primary tumors and metastases, however, a significant number of mutations are exclusive to the metastases of the studied patients.

The ratio of non-synonymous and synonymous mutations indicates a considerable number of driver genes

The number of non-synonymous (NS) and synonymous (S) mutations identified in the primary tumors of each patient are shown in [Table 2](#). NS:S ratios in four of the six studied primary tumors are significantly higher than the NS:S ratio of 2:1 predicted for non-selected passenger mutations. For the remaining two primary tumors, the numbers are probably too small to reach significance. The number of cancer driver mutations, conferring a selective advantage to the malignant cells, can be calculated as the number of non-synonymous mutations exceeding the expected ratio of 2:1. With reservations for our assumptions, the number of driver genes in the primary tumors included in our study varies between 3 and 145 ([S9 Table](#)). The NS:S ratios for ALN metastases specific mutations collectively reaches statistical significance ([Table 3](#)), while the mutations specific to the asynchronous metastases do not reach the normally accepted statistical significance level of 5%.

Recurrently mutated genes in metastatic progression

A number of genes are recurrently mutated within individual patient samples and across the six studied patients as seen in [Tables 4](#) and [5](#), respectively. Some of the genes are already established as cancer related genes as they are present in the Catalogue Of Somatic Mutations In Cancer (COSMIC) Cancer Gene Census list (<http://cancer.sanger.ac.uk/cancergenome/projects/census/>) while the remaining genes may include novel cancer driving genes.

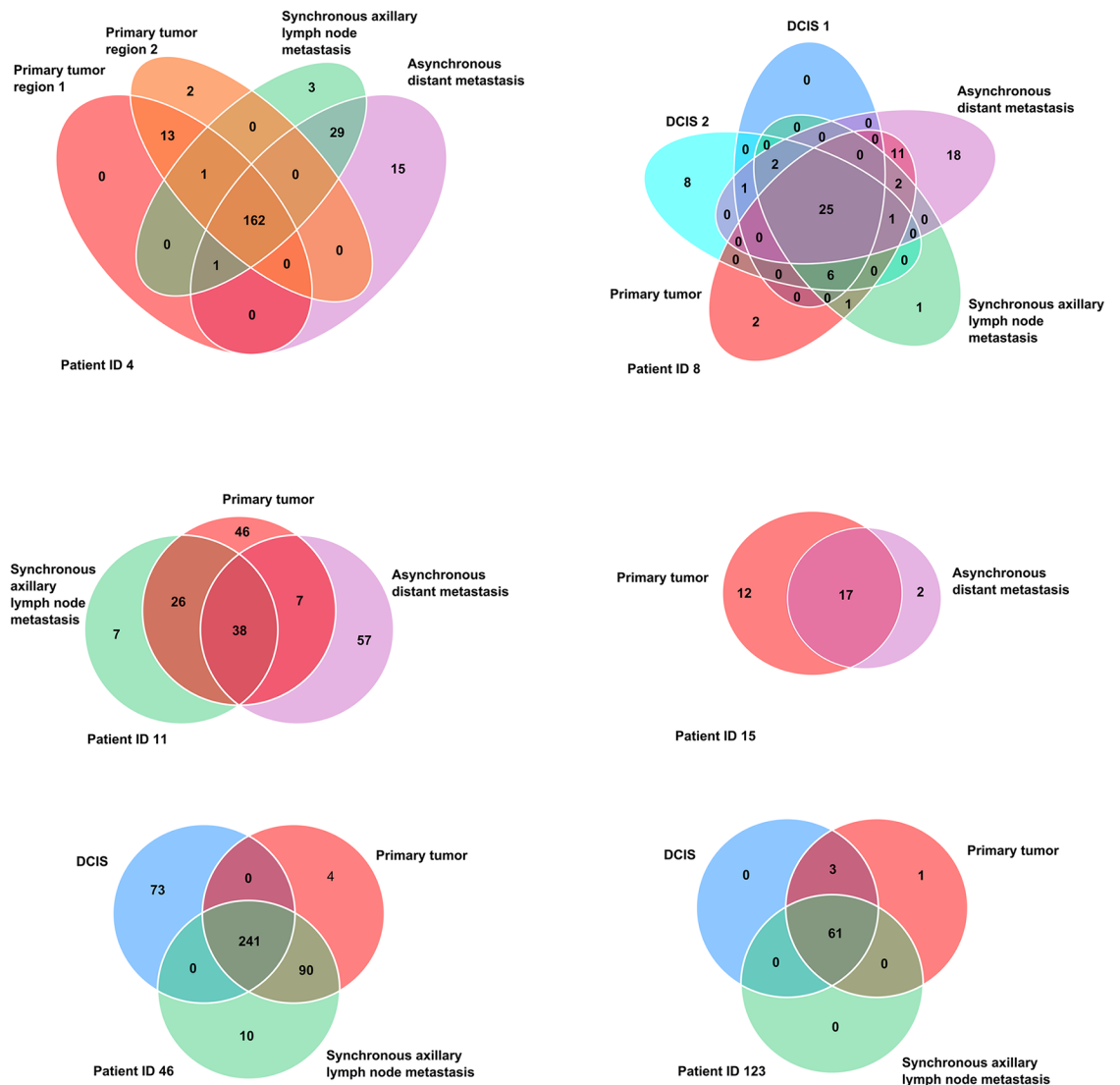


Fig 1. Genomic concordance. Venn diagrams depicting the genomic concordance of non-synonymous and splice site mutations between different steps of progression in the six studied patients.

<https://doi.org/10.1371/journal.pone.0189887.g001>

Table 2. Non-synonymous and synonymous mutations present in the primary tumors.

| | PT ID 4 | PT ID 8 | PT ID 11 | PT ID 15 | PT ID 46 | PT ID 123 |
|----------------|---------|---------|----------|----------|-----------------------|-----------|
| Non-synonymous | 177 | 48 | 117 | 29 | 335 | 65 |
| Synonymous | 47 | 16 | 42 | 13 | 95 | 21 |
| Ratio | 3.76 | 3.0 | 2.78 | 2.23 | 3.52 | 3.09 |
| P-value | 0.00003 | 0.097 | 0.036 | 0.44 | 2.08×10^{-7} | 0.047 |

P-values are calculated by one-tailed binomial test.

<https://doi.org/10.1371/journal.pone.0189887.t002>

Table 3. Non-synonymous and synonymous mutations specific for mutations in ALN metastases and asynchronous distant metastases, respectively, collectively for the six studied patients.

| | ALN metastasis specific mutations | Asynchronous distant mutation specific mutations |
|----------------|-----------------------------------|--|
| Non-synonymous | 50 | 92 |
| Synonymous | 15 | 35 |
| Ratio | 3.33 | 2.62 |
| P-value | 0.049 | 0.097 |

P-values are calculated by one-tailed binomial test.

<https://doi.org/10.1371/journal.pone.0189887.t003>

Table 4. Recurrently mutated genes within individual patient samples.

| | Cosmic CGC | Patient ID 4 | | | | Patient ID 8 | | | | | Patient ID 11 | | | Patient ID 15 | | Patient ID 46 | | | Patient ID 123 | | |
|----------|------------|--------------|------|------|----|--------------|--------|----|------|----|---------------|------|----|---------------|----|---------------|----|------|----------------|----|------|
| Gene | | PT 1 | PT 2 | ALNM | DM | DCIS 1 | DCIS 2 | PT | ALNM | DM | PT | ALNM | DM | PT | DM | DCIS | PT | ALNM | DCIS | PT | ALNM |
| MUC4 | | | | | | | | | | | | 6x | 6x | x | | | | | | | |
| FREM2 | | 3x | 3x | | | | | | | | | | | | | | | | | | |
| BRCA2 | yes | 2x | 2x | 2x | 2x | | | | | | | | | | | | | | | | |
| TTN | | | | | | | | | | | | | | | | x | x | 2x | | | |
| USHBP1 | | | | | | | | | | | | | 3x | | | | | | | | |
| WAC | | | | | | | | | | | | | | | | 3x | 3x | 3x | | | |
| XIRP2 | | | | | | | | | | | | | 3x | | | | | | | | |
| AKAP9 | yes | | | | | | | | | | | | | | | 2x | x | x | | | |
| ARHGAP21 | | 2x | 2x | 2x | 2x | | | | | | | | | | | | | | | | |
| ARMC5 | | 2x | 2x | 2x | 2x | | | | | | | | | | | | | | | | |
| BRD2 | | | | | | | | | | | | | | | | x | 2x | 2x | | | |
| C1orf63 | | 2x | 2x | 2x | 2x | | | | | | | | | | | | | | | | |
| CAMK2A | | 2x | 2x | 2x | 2x | | | | | | | | | | | | | | | | |
| F5 | | 2x | 2x | 2x | 2x | | | | | | | | | | | | | | | | |
| FCGBP | | | | | | | | | | | | | | | | x | | 2x | | | |
| IL6ST | yes | | | | | | | | | | 2x | x | x | | | | | | | | |
| KIAA1731 | | | | | | | | | | | 2x | 2x | 2x | | | | | | | | |
| LRP1 | | | | | | | | | | | | | | | | 2x | 2x | 2x | | | |
| METTL22 | | | | | | | | | | | | | | | | 2x | 2x | 2x | | | |
| PCDHB16 | | | | | | | | | | | 2x | | 2x | | | | | | | | |
| PLAT | | | | | | | | | | | | | | | | 2x | 2x | 2x | | | |
| PTPRK | yes | | | | | | | | | | | | | | | 2x | 2x | 2x | | | |
| RIC8A | | | | | | | | | | | | | | | | 2x | 2x | 2x | | | |
| RUNX1 | yes | | | | | | | | | | | | | | | 2x | 2x | 2x | | | |
| TFRC | yes | | | | | | | | | | | | | | | x | 2x | 2x | | | |
| TIAM2 | | | | | | | | | | | | | | | | | | 2x | | | |
| UGGT2 | | | | | | | | | | | | | | | | x2 | x2 | x2 | | | |
| ZNF469 | | | | | | | | | | | 2x | | | | | | | | | | |
| ABCA13 | | | | | | | | | | | | | | | | | | | 3x | 3x | 3x |

Only non-synonymous and splice site mutations are included. Cosmic CGC: Included in the Cosmic Cancer Gene Census. x: one mutation. 2x: two mutations. 3x: three mutations. 6x: six mutations. DCIS: ductal carcinoma in situ. DM: asynchronous distant metastasis. PT: patient. ALNM: axillary lymph node metastasis.

<https://doi.org/10.1371/journal.pone.0189887.t004>

Table 5. Recurrently mutated genes across patients.

| | Cosmic CGC | Patient ID 4 | | | | Patient ID 8 | | | | | Patient ID 11 | | | Patient ID 15 | | Patient ID 46 | | | Patient ID 123 | | | |
|----------|------------|--------------|------|------|----|--------------|--------|----|------|----|---------------|------|----|---------------|----|---------------|----|------|----------------|----|------|--|
| Gene | | PT 1 | PT 2 | ALNM | DM | DCIS 1 | DCIS 2 | PT | ALNM | DM | PT | ALNM | DM | PT | DM | DCIS | PT | ALNM | DCIS | PT | ALNM | |
| TP53 | yes | | | | | x | x | x | x | x | x | x | x | | | x | x | x | | | | |
| KIAA1033 | | | | | | x | x | x | x | x | | | | | | x | x | x | x | x | x | |
| TNXB | | | | | | | | | | | x | x | | | | x | x | x | x | x | x | |
| WDFY4 | | x | x | x | x | | x | x | x | x | | | | | | | | | | | | |
| PCDHGA1 | | x | x | x | x | | | | | | | | | | | x | x | x | | | | |
| MAN2C1 | | x | x | x | x | | | | | | | | | | | | x | x | | | | |
| MYO3A | | x | x | x | x | | | | | | | | | | | x | x | x | | | | |
| RUNX1 | yes | x | x | x | x | | | | | | | | | | | 2x | 2x | 2x | | | | |
| BRCA2 | yes | 2x | 2x | 2x | 2x | | | | | | | | | | | x | x | x | | | | |
| YY1AP1 | | x | x | x | x | | | | | | | | | | | x | x | x | | | | |
| STK4 | | x | x | x | x | | | | | | | | | | | x | x | x | | | | |
| LRRK1 | | x | x | x | x | | | | | | | | | | | | | | x | x | x | |
| SLC41A2 | | x | x | x | x | | | | | | | | | | | | x | x | | | | |
| CDH23 | | x | x | x | x | | | | | | | | x | | | | | | | | | |
| ZNF827 | | x | x | x | x | | | | | | | | | | | | | | x | x | | |
| ABCA13 | | | | x | x | | | | | | | | | | | | | | 3x | 3x | 3x | |
| LTN1 | | | | x | x | | | | | | | | | | | | | | x | x | x | |
| UNC80 | | | | x | x | | | | | | | | | | | | x | x | | | | |
| PIK3CA | yes | | | | | | | | | | x | x | x | | | x | x | x | | | | |
| APLF | | | | | | | | | | | x | x | | | | | | | x | x | x | |
| BAI3 | | | | | | | | | | | x | | | | | x | x | x | | | | |
| C4orf21 | | | | | | | | | | | x | | x | | | | | | x | x | x | |
| DCC | | | | | | | | | | | | | | | x | | | x | | | | |
| DNAH11 | | | | | | | | | | | | | | x | x | x | x | x | | | | |
| DYNC2H1 | | | | | | | | | | | x | x | x | | | x | x | x | | | | |
| KLHL32 | | | | | | | | | | | x | x | x | | | x | | | | | | |
| NXNL2 | | | | | | | | | | | x | x | x | | | | | | x | x | x | |
| PTPN14 | | | | | | | | | | | x | x | x | | | x | x | x | | | | |
| ROS1 | yes | | | | | | | | | | x | | | | | x | x | x | | | | |
| SGCE | | | | | | | | | | | | | | | | x | x | x | x | x | x | |
| SON | | | | | | | | | | | x | x | x | | | x | x | x | | | | |
| TLN2 | | | | | | | | | | | x | x | | | | | x | x | | | | |
| UTP20 | | | | | | | | | | | | | | x | | | x | x | | | | |
| VWF | | | | | | | | | | | | x | | x | x | | | | | | | |
| FLG | | | | | | | | | | | | | x | | | x | x | x | | | | |
| UBE2O | | | | | | | | | | | | | x | | | | x | x | | | | |

Includes only non-synonymous and splice site mutations. Cosmic CGC: Included in the Cosmic Cancer Gene Census. x: one mutation. 2x: two mutations. 3x: three mutations. DCIS: ductal carcinoma in situ. DM: asynchronous distant metastasis. PT: patient. ALNM: axillary lymph node metastasis.

<https://doi.org/10.1371/journal.pone.0189887.t005>

Different gene sets are mutated at different steps of malignant progression

The genes affected by non-synonymous and splice site mutations in the six studied patients were divided into three categories based on the steps of malignant progression in which they appear. The genes included in Categories 1–3 are listed in [S10 Table](#). Pathway analysis on the three categories of genes revealed that different pathways are involved in the different steps of

Table 6. Results from overlap analyses, Category 1. Pathway analysis of genes mutated exclusively in DCIS and primary tumors, 147 in total.

| Pathways | Genes in overlap | p-value | FDR q-value |
|--|------------------|-----------|-------------|
| KEGG Homologous recombination (28) | 4 | 1.94 E -6 | 3.6 E -4 |
| KEGG Steroid hormone biosynthesis (55) | 3 | 7.45 E -4 | 6.93 E -2 |
| KEGG Primary bile acid biosynthesis (16) | 2 | 1.18 E -3 | 7.34 E -2 |
| KEGG Mismatch repair (23) | 2 | 2.46 E -3 | 1.14 E -1 |
| KEGG Dilated cardiomyopathy (92) | 3 | 3.27 E -3 | 1.22 E -1 |

(#): number of genes in pathway. FDR: false discovery rate.

<https://doi.org/10.1371/journal.pone.0189887.t006>

malignant progression. In Category 1, including 147 genes found to be mutated exclusively in pre-invasive tissue or primary tumors, the top five KEGG pathways included Homologous recombination and Mismatch repair pathways among others, as shown in Table 6.

Category 2, including 606 genes mutated in primary tumors and matched metastases, is significantly enriched for genes on various cancer related pathways, as seen in Table 7. Pathway analysis on the 129 metastasis specific genes in Category 3 reveals that the top three pathways, although not reaching statistical significance levels, are KEGG Adherens junction, KEGG Ubiquitin mediated proteolysis and KEGG Wnt signaling pathway Table 8. These pathways are likely to be key participants in the metastatic process. Three genes, *NLK* (PTID 8), *CREBBP* (PTID 4), *CTNN2A* (PTID11) are involved in the KEGG Adherens junction pathway and thus this pathway is affected in the distant metastases of three of the patients, as seen in Fig 2. Three

Table 7. Results from overlap analyses, Category 2. Pathway analysis of genes mutated in primary tumors and corresponding metastases, 606 in total.

| Pathways | Genes in overlap | p-value | FDR q-value |
|---|------------------|-----------|-------------|
| KEGG Neutrophin signaling pathway (126) | 13 | 1.41 E -8 | 2.62 E -6 |
| KEGG Chronic myeloid leukemia (73) | 10 | 4.35 E -8 | 4.05 E -6 |
| KEGG Pathways in cancer (328) | 19 | 1.02 E -7 | 6.35 E -6 |
| KEGG Endometrial cancer (52) | 8 | 3.94 E -7 | 1.75 E -5 |
| KEGG Focal adhesion (201) | 14 | 5.51 E -7 | 1.75 E -5 |
| KEGG Steroid hormone biosynthesis (55) | 8 | 6.16 E -7 | 1.75 E -5 |
| KEGG MAPK signaling pathway (267) | 16 | 6.6 E -7 | 1.75 E -5 |
| KEGG Glioma (65) | 8 | 2.28 E -6 | 4.83 E -5 |
| KEGG ERBB signaling pathway (87) | 9 | 2.34 E -6 | 4.83 E -5 |
| KEGG Complement and coagulation cascades (69) | 8 | 3.6 E -6 | 6.7 E -5 |
| KEGG Non-small cell lung cancer (54) | 7 | 6.93 E -6 | 1.17 E -4 |
| KEGG Insulin signaling pathway (137) | 10 | 1.51 E -5 | 2.35 E -4 |
| KEGG Colorectal cancer (62) | 7 | 1.76 E -5 | 2.52 E -4 |
| KEGG Calcium signaling pathway (178) | 11 | 2.74 E -5 | 3.64 E -4 |
| KEGG Thyroid cancer (29) | 5 | 3.58 E -5 | 4.44 E -4 |
| KEGG Pancreatic cancer (70) | 7 | 3.91 E -5 | 4.55 E -4 |
| KEGG GnRH signaling pathway (101) | 8 | 6.02 E -5 | 6.33 E -4 |
| KEGG B cell receptor signaling pathway (75) | 7 | 6.12 E -5 | 6.33 E -4 |
| KEGG Acute myeloid leukemia (60) | 6 | 1.4 E -4 | 1.37 E -3 |
| KEGG Prostate cancer (89) | 7 | 1.81 E -4 | 1.69 E -3 |

(#): number of genes in pathway. FDR: false discovery rate.

<https://doi.org/10.1371/journal.pone.0189887.t007>

Table 8. Results from overlap analyses, Category 3. Pathway analysis of genes mutated exclusively in metastases, 129 in total.

| Pathways | Genes in overlap | p-value | FDR q-value |
|---|------------------|-----------|-------------|
| KEGG Adherens junction (75) | 3 | 1.26 E -3 | 2.34 E -1 |
| KEGG Ubiquitin mediated proteolysis (138) | 3 | 7.03 E -3 | 4.43 E -1 |
| KEGG Wnt signaling pathway (151) | 3 | 8.99 E -3 | 4.43 E -1 |

(#): number of genes in pathway. FDR: false discovery rate.

<https://doi.org/10.1371/journal.pone.0189887.t008>

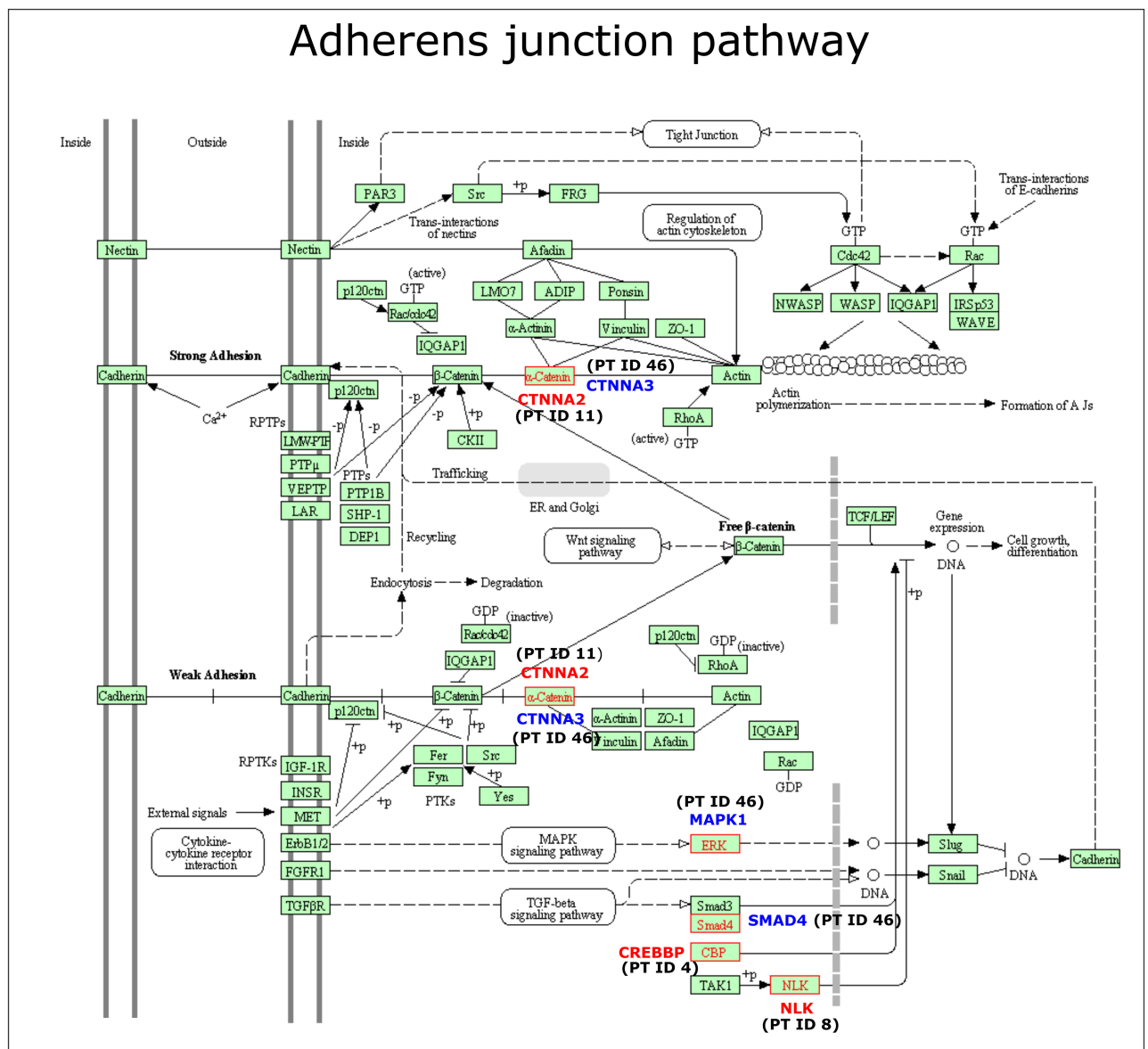


Fig 2. KEGG Adherens junction pathway, which is affected exclusively in the metastases of three of the studied patients (gene names in red), and affected by shared mutations between primary tumor and metastasis in one patient (gene names in blue). CTNNA2 and CTNNA3 are both encoding α -catenins. Patient IDs are in brackets.

<https://doi.org/10.1371/journal.pone.0189887.g002>

genes, *MAPK1*, *SMAD4* and *CTNNA3*, also belonging to the Adherens junction pathway are affected by mutations in both primary tumor and metastasis of a fourth of the studied patients (PTID 46). Pathway analysis including genes mutated in both Category 2 and Category 3 reveals the Adherens junction pathway to be significantly affected (FDR q value 6.08×10^{-3}) in the primary tumors and metastases of the studied patients.

Putative novel drivers of metastatic progression can be found among genes affected by metastasis specific mutations and mutations shared between primary tumors and metastases

Exclusively in the metastases, 142 non-synonymous and splice site mutations were found. Among these, 45 mutations in 43 genes are classified as putative progression drivers as they are affected by splice site, stopgain or frameshift mutations or a missense mutation classified as an iCAGES driver mutation. The putative drivers of progression among the genes mutated exclusively in the metastases of the studied patients are listed in Table 9. Some of the genes are already present in the Cancer Gene Census list or KEGG cancer pathway (http://www.genome.jp/kegg-bin/show_pathway?hsa05200) while other genes may represent novel drivers of malignant progression. Several of the genes are likely cancer progression genes, based on literature review, while other genes have not (yet) been described in relation to cancer.

Category 2, including genes affected by shared mutations between primary tumors and metastases, includes 692 mutations. Among these, 206 mutations are classified as putative metastasis progression driver genes as they are affected by splice site, stopgain or frameshift mutations or a nonsynonymous missense mutation classified as an iCAGES driver mutation. The putative driver genes of metastatic progression from Category 2 can be found in S11 Table.

Discussion

The present study reports substantial variation in the number of mutations within the coding region and varying mutational concordance between different steps of malignant progression in the studied breast cancer patients.

A key challenge in cancer genetics is to distinguish between driver and passenger mutations. The identified high NS:S ratios in our study imply positive selection of non-synonymous mutations in the studied primary tumors and thereby indicate that a surprisingly large proportion of the identified genes have functional significance. This is in concordance with significant enrichment in Category 2 of genes involved in many cancer related pathways. The number of calculated driver mutations in the primary tumors included in our study varies greatly, ranging between 3 and 145. Other studies have attempted to estimate the number of driver mutations in solid tumors like breast cancer and suggested up to 20 driver mutations [25,26]. Supporting the notion of many driver genes, it is estimated, that each driver mutation confers only a small selective growth advantage to the cell in the order of 0.4% [27]. Progression from early tumor stages to metastatic lesions is an evolutionary process and metastatic capacity most likely results from multiple alterations, each providing a slight selective advantage at the different steps of metastasis.

We present putative novel drivers of metastatic progression from the category of genes mutated exclusively in the metastases of the studied patients (Category 3). One could argue that metastasis promoting mutations may also be present in the mutations shared between primary tumors and metastases (Category 2) as it seems likely that metastatic abilities, at least the ones required for the early steps of the metastatic process, metastasis initiation genes, are present in the cells prior to dissemination from the primary tumor. However, only clonally

Table 9. Putative drivers of metastatic progression from Category 3, metastasis specific mutations.

| PT ID 4 | Gene | CytoBand | Mutation type | cDNA change | AA change | Category | iCAGES | ALNM BAF | DM BAF |
|----------|------------|----------|---------------|----------------|--------------|----------|--------|----------|--------|
| | LAMB3 | 1q32.2 | S | c.1132+2T>G | | | | x | x |
| | DUSP10 | 1q41 | NS | c.335A>C | p.Q112P | | Yes | x | x |
| | IL1RAP | 3q28 | FS del | c.295_302del | p.99_101del | | | x | x |
| | ABCA13 | 7p12.3 | FS del | c.7112delG | p.R2371fs | | | x | x |
| | CREBBP | 16p13.3 | NS | c.4357C>A | p.Q1453K | CGC | Yes | x | x |
| | GTF2F1 | 19p13.3 | NS | c.808G>C | p.E270Q | | Yes | x | x |
| | BCL6B | 17p13.1 | FS del | c.1176_1185del | p.392_395del | | | x | x |
| | ZNF185 | Xq28 | S | c.1971+2T>A | | | | x | x |
| | ACADM | 1p31.1 | NS | c.271A>T | p.T91S | | Yes | x | |
| | ST6GALNAC3 | 1p31.1 | SG | c.874A>T | p.K292X | | | x | |
| | ZAP70 | 2q11.2 | NS | c.920C>T | p.P307L | | Yes | | x |
| | MYO7A | 11q13.5 | NS | c.3126G>T | p.W1042C | | Yes | | x |
| | CDH5 | 16q21 | NS | c.1738G>A | p.E580K | | Yes | | x |
| | PPP2R1A | 19q13.41 | NS | c.28C>A | p.L10M | CGC | Yes | | x |
| | WDR52 | 3q13.2 | FS del | c.2513delA | p.N838fs | | | | x |
| | BRD8 | 5q31.2 | SG | c.1921G>T | p.E641X | | | | x |
| PT ID 8 | NCKAP5 | 2q21.2 | S | c.1757-2A>G | | | | | x |
| | VCAN | 5q14.3 | NS | c.2539G>C | p.E847Q | | Yes | | x |
| | ARID1B | 6q25.3 | NS | c.3607G>T | p.A1203S | | Yes | | x |
| | OR1K1 | 9q33.2 | NS | c.160C>A | p.P54T | | Yes | | x |
| | NLK | 17q11.2 | NS | c.230C>T | p.A77V | | Yes | | x |
| | DOCK6 | 19p13.2 | NS | c.2338C>A | p.L780M | | Yes | | x |
| | GSG1L | 16p12.1 | SG | c.507C>A | p.C169X | | | | x |
| PT ID 11 | SPSB1 | 1p36.22 | NS | c.442C>T | p.R148W | | Yes | | x |
| | OR2M4 | 1q44 | NS | c.745G>A | p.G249R | | Yes | | x |
| | CTNNA2 | 2p12 | NS | c.625G>A | p.A209T | KEGG | Yes | | x |
| | ITPR1 | 3p26.1 | NS | c.7915G>A | p.E2639K | | Yes | | x |
| | PTPN13 | 4q21.3 | NS | c.3015G>T | p.M1005I | | Yes | | x |
| | GPRC6A | 6q22.1 | NS | c.1637G>T | p.R546I | | Yes | | x |
| | CSPP1 | 8q13.2 | FS del | c.2032delA | p.K678fs | | | | x |
| | UBE3B | 12q24.11 | NS | c.3073G>C | p.E1025Q | | Yes | | x |
| | HS3ST3A1 | 17p12 | NS | c.1132G>A | p.E378K | | Yes | | x |
| | UBE2O | 17q25.1 | NS | c.1661C>T | p.S554L | | Yes | | x |
| | PTGIS | 20q13.13 | NS | c.907C>T | p.P303S | | Yes | | x |
| | PI4KA | 22q11.21 | NS | c.1939G>A | p.V647M | | Yes | | x |
| | APOL5 | 22q12.3 | S | c.142+1G>A | | | | | x |
| | ZNRF3 | 22q12.1 | NS | c.1291C>G | p.H431D | | Yes | x | |
| | VWF | 12p13.31 | NS | c.1471C>T | p.R491C | | Yes | x | |
| PT ID 15 | DCC | 18q21.2 | NS | c.151A>G | p.T51A | KEGG | Yes | | x |
| PT ID 46 | TMPRSS11A | 4q13.2 | SG | c.282G>A | p.W94X | | | x | |
| | TIAM2 | 6q25.3 | NS | c.1627G>T | p.G543C | | Yes | x | |
| | TIAM2 | 6q25.3 | NS | c.1671C>A | p.F557L | | Yes | x | |
| | A2M | 12p13.31 | NS | c.943G>A | p.E315K | | Yes | x | |
| | DCC | 18q21.2 | NS | c.3242G>C | p.G1081A | KEGG | Yes | x | |
| | FCGBP | 19q13.2 | SG | c.14279C>G | p.S4760X | | | x | |

AA change: amino acid change. ALNM: axillary lymph node metastasis. DM: asynchronous distant metastasis. BAF: B allele frequency. Del: deletion. CGS: Cosmic Cancer Gene Census. FS: frameshift. NS: non-synonymous missense. S: splicing. SG: stopgain. KEGG: KEGG cancer pathway.

<https://doi.org/10.1371/journal.pone.0189887.t009>

expanded mutations are detectable in a study like the present and therefore, a detected mutation either confers a selective advantage or is a passenger in a successful clone. Hence, for a mutation in Category 2 to be a driver of metastatic progression it should be advantageous both at the primary tumor site and in the metastatic setting. This is indeed possible for some metastatic abilities such as invasion or angiogenesis. Thus, Category 2 most likely also contains metastasis progression drivers.

Different gene sets are affected by mutations at different steps of malignant progression. In Category 1, the top five KEGG pathways included Homologous recombination and Mismatch repair. These pathways are intuitively relevant for carcinogenesis, the early stages of malignancy. Category 2 is significantly enriched for genes participating in various cancer related pathways. The Adherens junction pathway is affected by mutations exclusively in the metastases of three of the studied patients. Adherens junctions are the most common type of intercellular adhesion and limits cell movement and proliferation and are therefore likely to play a key role in the metastatic process. Metastasis-enabling mutations may, as discussed, be present already within the primary tumor. Hence, it seems relevant to include both Category 2 and Category 3 genes in a pathway analysis, revealing the Adherens junction pathway to be significantly affected in the primary tumors and metastases of the studied patients.

Recurrently mutated genes among the studied patients are highly likely cancer drivers. Three genes, *BRCA2*, *RUNX1* and *ABCA13* are affected by recurrent mutations both within patients and among patients and are previously described in relation to cancer [28–30]. The established cancer gene *PIK3CA* [31] is affected in all tumor steps of two of the studied patients. Focusing on metastases, the *ABCA13*, *DCC* and *TIAM2* genes deserve mention. The *ABCA13* gene is, in addition to mutations in all tumor steps of PTID 123, affected by a frame-shift deletion exclusively in the metastases of PTID 4. An association has been found between ATP-binding cassette transporter genes like *ABCA13* and outcome in breast cancer patients, most likely due to their role in drug resistance [30]. The *DCC* gene, mutated exclusively in metastases of two of the studied patients (PTID 15 and 46), most likely plays a role in the metastatic phenotype. Studies in *Drosophila* have suggested that the *DCC* gene functions as an invasive tumor suppressor [32,33]. In a murine model of p53 deficient mammary carcinoma cells it has been reported that additional loss of *DCC* promotes metastasis formation without affecting the primary tumor phenotype [34] suggesting that the gene limits survival of disseminated tumor cells. The *TIAM2* gene is affected by two non-synonymous mutations exclusively in the metastasis of PT ID 46. *TIAM2S* expression is reported to be positively associated with metastatic phenotype of hepatocellular carcinoma cells and the gene product reported to promote growth and invasiveness [35]. *In vivo* studies revealed that *TIAM2S* expression resulted in up-regulation of N-cadherin and vimentin and redistribution of E-cadherin [35]. Thus, the *TIAM2* gene is found to function as an oncogene promoting epithelial-to-mesenchymal transition. In order for the gene to function as a progression driver in the metastatic cells in our study, the non-synonymous mutations identified in the gene should be activating mutations.

A number of genes are found to be recurrently mutated within individual patient samples. This phenomenon could be suspected to result from false positive calls. However, in this study, validation includes sequencing with a mean read depth of 465 x and called positions were manually curated, ensuring high quality of the reported findings. Whether recurrently mutated genes within a tumor specimen are situated in cis or in trans and whether they originate from the same or different cancer cell subclones cannot be established. Two inactivating mutations located at different alleles within the same cancer cells result in a total inactivation of the gene. Conversely, if two cancer subclones are affected by different mutations in the same gene this again suggests a strong selective advantage of mutations in the gene.

From the list of putative drivers of metastatic progression found only among the metastasis specific mutations the *CREBBP*, *BCL6B* and the *ZNF185* genes are the most notable. The *CREBBP* gene, mutated exclusively in the metastases of PTID 4, is an epigenetic modifier acting as a transcriptional coactivator through acetylation of histone proteins, thereby securing transcription of genes, including tumor suppressor genes and has thus been suggested as tumor suppressor [36]. The *BCL6B* gene, affected by a frameshift deletion exclusively in both metastases of PTID 4, is recently reported a novel tumor suppressor gene in hepatocellular carcinoma [37]. The *BCL6B* gene functions as a sequence-specific transcriptional repressor in the nucleus and is ubiquitously expressed in human tissue. Stable expression of the gene in hepatocellular cell lines was found to suppress cell migration and invasion and significantly reduced the incidence and severity of lung metastases in a mouse model [37]. The anti-metastatic effect of *BCL6B* was mediated by up-regulation of cell adhesion molecules like E-cadherin and down-regulation of the angiogenesis gene *VEGFA* [37]. The *ZNF185* gene, affected by a splicing mutation specifically in both metastases of PTID 4, is suggested to function as a tumor suppressor by associating with the actin-cytoskeleton and is reported to be associated with metastatic progression in colon and prostate cancer [38,39].

The studied cancer genomes most likely represent highly aggressive and treatment insensitive cases and the reported mutational spectrum is highly influenced by the selective pressures provided by treatment. Some of the mutations may play a role in therapy resistance. Mutations in the *RUNX1* gene is previously reported to correlate with aromatase inhibition resistance [40]. Our study supports this finding as, in two of the six studied patients, the *RUNX1* gene is affected by mutations in all tumor steps and the patients experienced progression of the disease in spite of treatment with the aromatase inhibitor Letrozole.

The prioritization among missense mutations for the identification of cancer driver genes is extremely challenging and no software tool can perform the distinction flawlessly. Thus, the use of the iCAGES software is just one way one could address this task.

The present study, like most other, focuses on non-synonymous mutations, as synonymous mutations are widely considered nonfunctional in cancer. However, a relatively recent study provides evidence that such silent mutations can actually act as oncogenic drivers by altering transcript splicing and therefore affect protein function [41]. In contrast to what was previously known, it is found that natural selection also acts on synonymous sites as it was found that oncogenes, in addition to being enriched for activating missense mutations, were also enriched for synonymous mutations compared to non-cancer genes [41]. A strong association was found between synonymous mutations and differential exon usage profiles in the most recurrently mutated oncogenes. Generally, tumor suppressor genes did not display the same phenomenon, except *TP53* which also had recurrent synonymous mutations that, in contrast to those in oncogenes, were adjacent to splice sites and inactivate them [41]. The study found synonymous mutations to be nonrandomly distributed across the cancer genome and that they preferentially targeted evolutionary conserved sites. Hence, synonymous mutations might confer a selective advantage to the malignant cells. In our study, we do not find evidence of selective forces acting on synonymous mutations, however, this does not preclude that a few of the identified synonymous mutations actually do function as a progression driver.

In summary, we report substantial mutational discordance between different steps of malignant progression in the studied breast cancer patients. Putative novel drivers of malignant progression are reported among the genes mutated exclusively in the metastases and among the genes shared between the primary tumors and metastases. Most notable are the *DCC*, *TIAM2*, *CREBBP*, *BCL6B* and the *ZNF185* genes, mutated exclusively in the metastases of the studied patients and highly likely driver genes of metastatic progression. High NS:S ratios reveal positive selection of non-synonymous mutations and that more than a few driver genes confer a

selective advantage in the studied primary tumors. Different genes and pathways are involved at different stages of breast cancer. The Adherens junction pathway is affected in four of the six studied patients and this pathway most likely plays a vital role in the metastatic process. The considerable amount of additional mutations in the asynchronous metastases in several of the studied patients stresses the importance of molecular profiling of metastatic tissue at recurrence of breast cancer in order to provide the optimal basis for personalized medicine.

Supporting information

S1 Table. Exome sequencing data.

(XLSX)

S2 Table. Mean coverage of validated positions.

(XLSX)

S3 Table. PT ID 4 validated positions in the coding region.

(XLSX)

S4 Table. PT ID 8 validated positions in the coding region.

(XLSX)

S5 Table. PT ID 11 validated positions in the coding region.

(XLSX)

S6 Table. PT ID 15 validated positions in the coding region.

(XLSX)

S7 Table. PT ID 46 validated positions in the coding region.

(XLSX)

S8 Table. PT ID 123 validated positions in the coding region.

(XLSX)

S9 Table. Calculations of number of driver mutations within the studied primary tumors.

(XLSX)

S10 Table. Genes included in Categories 1, 2 and 3, divided into the patients in which they are mutated.

(XLSX)

S11 Table. Putative driver genes of malignant progression from Category 2, mutations shared between primary tumors and metastases. Divided into the patients in which they are mutated.

(XLSX)

Acknowledgments

We thank Jette Møller, Marianne Käehne, Dorte Forsberg Jensen and Flemming Holm Bergholdt for excellent technical assistance.

Author Contributions

Conceptualization: Anne Bruun Krøigård, Martin Jakob Larsen, Mads Thomassen, Torben A. Kruse.

Data curation: Anne Bruun Krøigård, Martin Jakob Larsen, Anne-Vibeke Lænkholm.

Formal analysis: Anne Bruun Krøigård, Martin Jakob Larsen, Mads Thomassen, Torben A. Kruse.

Funding acquisition: Anne Bruun Krøigård.

Investigation: Anne Bruun Krøigård, Mads Thomassen.

Methodology: Anne Bruun Krøigård, Martin Jakob Larsen, Martin Bak, Torben A. Kruse.

Project administration: Anne Bruun Krøigård.

Resources: Ann S. Knoop, Jeanette Dupont Jensen.

Supervision: Jan Mollenhauer, Torben A. Kruse.

Writing – original draft: Anne Bruun Krøigård.

Writing – review & editing: Anne Bruun Krøigård.

References

1. Hanahan D, Weinberg RA. Hallmarks of Cancer: The Next Generation. *Cell*. 2011; 144:646–74. <https://doi.org/10.1016/j.cell.2011.02.013> PMID: 21376230
2. Yates LR, Campbell PJ. Evolution of the cancer genome. *Nat. Rev. Genet.* 2012; 13:795–806. <https://doi.org/10.1038/nrg3317> PMID: 23044827
3. Weinstein IB. Cancer. Addiction to oncogenes—the Achilles heel of cancer. *Science*. 2002; 297:63–4. <https://doi.org/10.1126/science.1073096> PMID: 12098689
4. Ostrow SL, Barshir R, DeGregori J, Yeger-Lotem E, Hershberg R. Cancer Evolution Is Associated with Pervasive Positive Selection on Globally Expressed Genes. *PLoS Genet.* [Internet]. 2014 [cited 2015 Jan 10];10. Available from: <http://www.ncbi.nlm.nih.gov/pmc/articles/PMC3945297/>
5. Vanharanta S, Massagué J. Origins of Metastatic Traits. *Cancer Cell*. 2013; 24:410–21. <https://doi.org/10.1016/j.ccr.2013.09.007> PMID: 24135279
6. Fidler IJ. Cancer biology is the foundation for therapy. *Cancer Biol. Ther.* 2005; 4:1036–9. PMID: 16222123
7. Hüseemann Y, Geigl JB, Schubert F, Musiani P, Meyer M, Burghart E, et al. Systemic spread is an early step in breast cancer. *Cancer Cell*. 2008; 13:58–68. <https://doi.org/10.1016/j.ccr.2007.12.003> PMID: 18167340
8. Marino N, Collins JW, Shen C, Caplen NJ, Merchant AS, Gökmen-Polar Y, et al. Identification and validation of genes with expression patterns inverse to multiple metastasis suppressor genes in breast cancer cell lines. *Clin. Exp. Metastasis*. 2014;
9. Hurst DR, Welch DR. Metastasis suppressor genes at the interface between the environment and tumor cell growth. *Int. Rev. Cell Mol. Biol.* 2011; 286:107–80. <https://doi.org/10.1016/B978-0-12-385859-7.00003-3> PMID: 21199781
10. Nguyen DX, Massagué J. Genetic determinants of cancer metastasis. *Nat. Rev. Genet.* 2007; 8:341–52. <https://doi.org/10.1038/nrg2101> PMID: 17440531
11. Hoadley KA, Siegel MB, Kanchi KL, Miller CA, Ding L, Zhao W, et al. Tumor Evolution in Two Patients with Basal-like Breast Cancer: A Retrospective Genomics Study of Multiple Metastases. *PLoS Med.* 2016; 13:e1002174. <https://doi.org/10.1371/journal.pmed.1002174> PMID: 27923045
12. Tang M-HE, Dahlgren M, Brueffer C, Tjitrowirjo T, Winter C, Chen Y, et al. Remarkable similarities of chromosomal rearrangements between primary human breast cancers and matched distant metastases as revealed by whole-genome sequencing. *Oncotarget*. 2015; 6:37169–84. <https://doi.org/10.18632/oncotarget.5951> PMID: 26439695
13. Krøigård AB, Larsen MJ, Lænkholm A-V, Knoop AS, Jensen JD, Bak M, et al. Clonal expansion and linear genome evolution through breast cancer progression from pre-invasive stages to asynchronous metastasis. *Oncotarget*. 2015; 6:5634–49. <https://doi.org/10.18632/oncotarget.3111> PMID: 25730902
14. Krøigård AB, Larsen MJ, Brasch-Andersen C, Lænkholm AV, Knoop AS, Jensen JD, Bak M, Mollenhauer J, Thomassen M, Kruse TA. Genomic Analyses of Breast Cancer Progression Reveal Distinct Routes of Metastasis Emergence. *Sci Rep*. 2017; 7:43813. <https://doi.org/10.1038/srep43813> PMID: 28276460

15. DePristo MA, Banks E, Poplin RE, Garimella KV, Maguire JR, Hartl C, et al. A framework for variation discovery and genotyping using next-generation DNA sequencing data. *Nat. Genet.* 2011; 43:491–8. <https://doi.org/10.1038/ng.806> PMID: 21478889
16. Shiraishi Y, Sato Y, Chiba K, Okuno Y, Nagata Y, Yoshida K, et al. An empirical Bayesian framework for somatic mutation detection from cancer genome sequencing data. *Nucleic Acids Res.* 2013; 41:e89. <https://doi.org/10.1093/nar/gkt126> PMID: 23471004
17. Christoforides A, Carpten JD, Weiss GJ, Demeure MJ, Von Hoff DD, Craig DW. Identification of somatic mutations in cancer through Bayesian-based analysis of sequenced genome pairs. *BMC Genomics.* 2013; 14:302. <https://doi.org/10.1186/1471-2164-14-302> PMID: 23642077
18. Hansen NF, Gartner JJ, Mei L, Samuels Y, Mullikin JC. Shimmer: detection of genetic alterations in tumors using next-generation sequence data. *Bioinformatics.* 2013; 29:1498–503. <https://doi.org/10.1093/bioinformatics/btt183> PMID: 23620360
19. Saunders CT, Wong WSW, Swamy S, Becq J, Murray LJ, Cheetham RK. Strelka: accurate somatic small-variant calling from sequenced tumor–normal sample pairs. *Bioinformatics.* 2012; 28:1811–7. <https://doi.org/10.1093/bioinformatics/bts271> PMID: 22581179
20. Koboldt DC, Zhang Q, Larson DE, Shen D, McLellan MD, Lin L, et al. VarScan 2: Somatic mutation and copy number alteration discovery in cancer by exome sequencing. *Genome Res.* 2012; 22:568–76. <https://doi.org/10.1101/gr.129684.111> PMID: 22300766
21. Kim S, Jeong K, Bhutani K, Lee JH, Patel A, Scott E, et al. Virmid: accurate detection of somatic mutations with sample impurity inference. *Genome Biol.* 2013; 14:R90. <https://doi.org/10.1186/gb-2013-14-r90> PMID: 23987214
22. Wang K, Li M, Hakonarson H. ANNOVAR: functional annotation of genetic variants from high-throughput sequencing data. *Nucleic Acids Res.* 2010; 38:e164–e164. <https://doi.org/10.1093/nar/gkq603> PMID: 20601685
23. Subramanian A, Tamayo P, Mootha VK, Mukherjee S, Ebert BL, Gillette MA, et al. Gene set enrichment analysis: A knowledge-based approach for interpreting genome-wide expression profiles. *Proc. Natl. Acad. Sci. U. S. A.* 2005; 102:15545–50. <https://doi.org/10.1073/pnas.0506580102> PMID: 16199517
24. Mootha VK, Lindgren CM, Eriksson K-F, Subramanian A, Sihag S, Lehar J, et al. PGC-1 α -responsive genes involved in oxidative phosphorylation are coordinately downregulated in human diabetes. *Nat. Genet.* 2003; 34:267–73. <https://doi.org/10.1038/ng1180> PMID: 12808457
25. Sjöblom T, Jones S, Wood LD, Parsons DW, Lin J, Barber TD, et al. The Consensus Coding Sequences of Human Breast and Colorectal Cancers. *Science.* 2006; 314:268–74. <https://doi.org/10.1126/science.1133427> PMID: 16959974
26. Beerenwinkel N, Antal T, Dingli D, Traulsen A, Kinzler KW, Velculescu VE, et al. Genetic Progression and the Waiting Time to Cancer. *PLoS Comput Biol.* 2007; 3:e225. <https://doi.org/10.1371/journal.pcbi.0030225> PMID: 17997597
27. Bozic I, Antal T, Ohtsuki H, Carter H, Kim D, Chen S, et al. Accumulation of driver and passenger mutations during tumor progression. *Proc. Natl. Acad. Sci. U. S. A.* 2010; 107:18545–50. <https://doi.org/10.1073/pnas.1010978107> PMID: 20876136
28. Tryggvadottir L, Olafsdottir EJ, Olafsdottir GH, Sigurdsson H, Johannsson OT, Bjorgvinsson E, et al. Tumour ploidy and survival in breast cancer patients with BRCA2 mutations. *Breast Cancer Res. Treat.* 2013; 140:375–84. <https://doi.org/10.1007/s10549-013-2637-4> PMID: 23857704
29. Ferrari N, Mohammed ZMA, Nixon C, Mason SM, Mallon E, McMillan DC, et al. Expression of RUNX1 Correlates with Poor Patient Prognosis in Triple Negative Breast Cancer. *PLoS ONE* [Internet]. 2014 [cited 2015 Feb 17]; 9. Available from: <http://www.ncbi.nlm.nih.gov/pmc/articles/PMC4072705/>
30. Hlaváč V, Brynychová V, Václavíková R, Ehrlichová M, Vrána D, Pecha V, et al. The expression profile of ATP-binding cassette transporter genes in breast carcinoma. *Pharmacogenomics.* 2013; 14:515–29. <https://doi.org/10.2217/pgs.13.26> PMID: 23556449
31. Zardavas D, Phillips WA, Loi S. PIK3CA mutations in breast cancer: reconciling findings from preclinical and clinical data. *Breast Cancer Res. BCR.* 2014; 16:201. <https://doi.org/10.1186/bcr3605> PMID: 25192370
32. VanZomeran-Dohm A, Sarro J, Flannery E, Duman-Scheel M. The Drosophila Netrin receptor frazzled/DCC functions as an invasive tumor suppressor. *BMC Dev. Biol.* 2011; 11:41. <https://doi.org/10.1186/1471-213X-11-41> PMID: 21672235
33. Duman-Scheel M. Deleted in Colorectal Cancer (DCC) Pathfinding: Axon Guidance Gene Finally Turned Tumor Suppressor. *Curr. Drug Targets.* 2012; 13:1445–53. PMID: 22876889
34. Krimpenfort P, Song J-Y, Proost N, Zevenhoven J, Jonkers J, Berns A. Deleted in colorectal carcinoma suppresses metastasis in p53-deficient mammary tumours. *Nature.* 2012; 482:538–41. <https://doi.org/10.1038/nature10790> PMID: 22358843

35. Chen J-S, Su I-J, Leu Y-W, Young K-C, Sun HS. Expression of T-cell lymphoma invasion and metastasis 2 (TIAM2) promotes proliferation and invasion of liver cancer. *Int. J. Cancer*. 2012; 130:1302–13. <https://doi.org/10.1002/ijc.26117> PMID: 21469146
36. Roy DM, Walsh LA, Chan TA. Driver mutations of cancer epigenomes. *Protein Cell*. 2014; 5:265–96. <https://doi.org/10.1007/s13238-014-0031-6> PMID: 24622842
37. Wang J, Dong L, Xu L, Chu ESH, Chen Y, Shen J, et al. B cell CLL/lymphoma 6 member B inhibits hepatocellular carcinoma metastases in vitro and in mice. *Cancer Lett*. 2014; 355:192–200. <https://doi.org/10.1016/j.canlet.2014.08.025> PMID: 25218345
38. Zhang J-S, Gong A, Young CYF. ZNF185, an actin–cytoskeleton-associated growth inhibitory LIM protein in prostate cancer. *Oncogene*. 2006; 26:111–22. <https://doi.org/10.1038/sj.onc.1209769> PMID: 16799630
39. FURUKAWA D, CHIJIWA T, MATSUYAMA M, MUKAI M, MATSUO E-I, NISHIMURA O, et al. Zinc finger protein 185 is a liver metastasis-associated factor in colon cancer patients. *Mol. Clin. Oncol*. 2014; 2:709–13. <https://doi.org/10.3892/mco.2014.298> PMID: 25054034
40. Ellis MJ, Ding L, Shen D, Luo J, Suman VJ, Wallis JW, et al. Whole-genome analysis informs breast cancer response to aromatase inhibition. *Nature*. 2012; 486:353–60. <https://doi.org/10.1038/nature11143> PMID: 22722193
41. Supek F, Miñana B, Valcárcel J, Gabaldón T, Lehner B. Synonymous mutations frequently act as driver mutations in human cancers. *Cell*. 2014; 156:1324–35. <https://doi.org/10.1016/j.cell.2014.01.051> PMID: 24630730